

Unsteady MHD Generalized Couette Flow in a Rotating Channel with Induced Magnetic Field, Hall Current and Periodically Magnetized Walls

Jitendra Kumar Singh*, Naveen Joshi and C. T. Srinivasa

Department of Mathematics
Vijayanagara Sri Krishnadevaraya University
Ballari-583105, India

Email: s.jitendrak@yahoo.com, joshi.naveen94@gmail.com,
srinivasact@rediffmail.com

(Received August 28, 2017)

Abstract: In this research work a mathematical analysis is presented for unsteady MHD generalized Couette flow of an incompressible and electrically conducting fluid in a rotating channel with induced magnetic field and Hall current. Both walls of the channel are magnetized and their magnetism is fluctuating periodically. The MHD flow through the parallel wall channel is developed due to an applied periodic pressure gradient and oscillatory movement of one of the walls of the channel. The solution of the flow governing coupled partial differential equations is obtained in closed form. To analyze the influences of various flow governing parameters, the numerical results for fluid velocity, induced magnetic field and skin friction at the moving wall are computed and presented through graphs and table. It is observed that Hall current raises the fluid velocity in the secondary flow direction in most of the upper part of the channel while this effect is upturned in the vicinity of the lower wall of the channel.

Keywords: Induced magnetic field, rotation, Hall current and magnetized wall.

AMS Mathematics Subject Classification: 76U05, 76W05.

Nomenclature

B'_x	induced magnetic field along x' -direction (T)	v	non-dimensional velocity along y' -direction
--------	--	-----	--

B'_y	induced magnetic field along y' -direction (T)	(x', y', z')	Cartesian coordinates
B_x	non-dimensional induced magnetic field in x' -direction	x	non-dimensional coordinate along channel wall
B_y	non-dimensional induced magnetic field in y' -direction	z	non-dimensional coordinate perpendicular to the channel wall
B_0	applied magnetic field (T)	α_m	magnetic interaction parameter
b'_0	constant	ε	constant
E	Ekmann number	μ_e	magnetic permeability
m	Hall current	ν	coefficient of viscosity (m^2 / s)
P_m	magnetic Prandtl number	ν_m	magnetic viscosity
p'	pressure	Ω	angular velocity
R	constant	ω'	frequency (s^{-1})
t'	time (s)	ω	non-dimensional frequency
t	non-dimensional time	ρ	fluid density (Kg / m^3)
U_0	constant velocity	σ	electrical conductivity (s / m)
u'	velocity along x' -direction (m / s)	τ_x	non-dimensional skin friction along x' -direction
u	non-dimensional velocity along x' -direction	τ_y	non-dimensional skin friction along y' -direction
v'	velocity along y' -direction (m / s)		

1. Introduction

Study of hydrodynamic duct or channel flows is significant due to its occurrence in many cosmological and geophysical problems and applications in energy systems, plasma aerodynamics and many engineering manufacturing processes. Couette flow is one of such a problem where flow is developed due to movement of the walls. In many wall driven flows, drag force and viscosity can be measured by using applications of Couette flows (Muzychka and Yovanovich¹). The MHD

flows developed due to an applied force together with the movement of the walls are named as generalized Couette flow or Couette-Hartmann flow. The study of generalized Couette flow in the presence of an applied magnetic field has drawn the considerable attention of the researchers during last few years due to its significant applications in engineering and technology such as nuclear engineering, electric and solar power generation technology, boundary layer control in polymer processing etc. The flow of electrically conducting fluid in the presence of an applied magnetic field produces a drag force whose nature is to suppress the fluid motion. This control mechanism is used in material processing. Stimulated from the industrial applications Agarwal², Soundalgekar³, Beg et al⁴, Singh et al^{5, 6} and Seth et al⁷ investigated the MHD generalized Couette flow problems by considering different geometries and approaches. In many industrial applications where the electromagnetic force is strong, there appear a current due to drifting of electrons in an ionized fluid. This current is called Hall current and it plays a prominent role in the determination of flow behaviors. The influence of Hall current on MHD channel or duct flows has been investigated by many researchers, namely, Nagy and Demendy⁸, Beg et al⁴, Jha and Apere⁹, Singh and Pathak¹⁰, Srinivasacharya and Kaladhar¹¹, Das et al¹², Seth and Singh¹³, Singh et al^{5, 6} and Seth et al⁷. It is worthy to note that in a rotating flow system, the force induces due to rotation (Coriolis force) is comparable to magnetic force (Lorentz force) and it also plays a vital role in determination flow characteristics. Motivated from these facts many researchers have been studied MHD flows in rotating system considering different aspects of the problems. Some recent contributions in MHD rotating flows are due to Nagy and Demendy⁸, Ghosh and Bhattacharjee¹⁴, Ansari et al¹⁵, Jha and Apere⁹, Singh and Pathak¹⁰, Seth and Singh¹³, Seth et al^{7, 16} and Singh et al⁶ in most of the MHD channel flows the channel walls are considered either non-conducting or infinitely conducting. Nagy and Demendy⁸ analyzed the combined Hall current and Coriolis force effects on MHD Hartmann flow with general wall condition. Subsequently, Ansari et al¹⁵ studied unsteady MHD flow of an electrically conducting fluid in a rotating channel with finitely conducting walls. They considered periodically fluctuating wall magnetism in their problem. Seth and Singh¹³ considered the Hall and wall conductance effects on mixed convection MHD flows in a rotating channel. Recently, Seth et al¹⁶ discussed the MHD oscillatory Hartmann flow of an incompressible and electrically conducting fluid in a rotating channel with periodically magnetized walls in the presence of a uniform transverse magnetic field.

In this intended research work, we analyzed the unsteady MHD

generalized Couette flow of an incompressible and electrically conducting fluid in a rotating channel with induced magnetic field and Hall current. We considered that the walls of the channel are magnetized and their magnetism is fluctuating periodically with time.

2. Mathematical Model and Its Solution

We consider fully developed MHD laminar flow of an incompressible and electrically conducting fluid within two parallel walls $(-\infty < x' < \infty, -\infty < y' < \infty)$ placed at $z' = -L$ and $z' = L$. The flow is permeated to pass through a magnetic field $\vec{B}(0, 0, B_0)$ applied along a direction perpendicular to the plane of the walls. Initially, the fluid and walls of the channel are considered to be at rest and the system is rotating rigidly with an angular velocity $\vec{\Omega}(0, 0, \Omega)$ about a direction normal to the channel walls. It is considered that the walls of the channel are magnetized periodically along x' -direction. The MHD flow through the channel is induced due to an applied periodic pressure gradient acting along x' -direction and oscillatory movement of the upper wall of the channel in its own plane along x' -direction. Since the flow is fully developed and laminar, so the all flow variables depend on z' and t' only. Under the above made assumptions and compatibility with continuity equation and solenoidal relation, the fluid velocity \vec{q} and the magnetic field \vec{B} may assume as $\vec{q} = (u', v', 0)$ and $\vec{B} = (B'_x, B'_y, B_0)$.

The flow governing equations for incompressible and electrically conducting fluid in a rotating channel with induced magnetic field and Hall current are described by

$$(2.1) \quad \frac{\partial u'}{\partial t'} - 2\Omega v' = -\frac{1}{\rho} \frac{\partial p'}{\partial x'} + \nu \frac{\partial^2 u'}{\partial z'^2} + \frac{B_0}{\rho \mu_e} \frac{\partial B'_x}{\partial z'},$$

$$(2.2) \quad \frac{\partial v'}{\partial t'} + 2\Omega u' = \nu \frac{\partial^2 v'}{\partial z'^2} + \frac{B_0}{\rho \mu_e} \frac{\partial B'_y}{\partial z'},$$

$$(2.3) \quad 0 = -\frac{1}{\rho} \frac{\partial}{\partial z'} \left\{ p' + \frac{1}{2\mu_e} (B'^2_x + B'^2_y + B^2_0) \right\},$$

$$(2.4) \quad \frac{\partial B'_x}{\partial t'} = B_0 \frac{\partial u'}{\partial z'} + \nu_m \frac{\partial^2 B'_x}{\partial z'^2} + \nu_m m \frac{\partial^2 B'_y}{\partial z'^2},$$

$$(2.5) \quad \frac{\partial B'_y}{\partial t'} = B_0 \frac{\partial v'}{\partial z'} + \nu_m \frac{\partial^2 B'_y}{\partial z'^2} - \nu_m m \frac{\partial^2 B'_x}{\partial z'^2}.$$

Equation (2.3) exhibits that the sum of the applied pressure and pressure due to magnetic field is constant along a direction normal to the wall of the channel. Since there is a net cross flow in y' -direction, so the pressure gradient term is absent in equation (2.2).

The boundary conditions specified for fluid velocity and induced magnetic field at the boundary walls of the channel are

$$(2.6) \quad \text{At } z' = -L : u' = v' = 0, \quad B'_x = b'_0 \left(1 + \varepsilon \left(e^{-i\omega t'} + e^{i\omega t'} \right) / 2 \right), \quad B'_y = 0.$$

$$(2.7) \quad \begin{cases} \text{At } z' = L : u' = U_0 \left(1 + \varepsilon \left(e^{-i\omega t'} + e^{i\omega t'} \right) / 2 \right), v' = 0, \\ B'_x = b'_0 \left(1 + \varepsilon \left(e^{-i\omega t'} + e^{i\omega t'} \right) / 2 \right), B'_y = 0. \end{cases}$$

To write flow governing equations (2.1)-(2.5) and boundary conditions (2.6) and (2.7) in non-dimensional form, we define the following non-dimensional quantities

$$(2.8) \quad \begin{cases} x = x' / L, \quad z = z' / L, \quad u = u' / U_0, \quad v = v' / U_0, \quad t = \Omega t', \quad \omega = \omega' / \Omega, \\ p' = \rho U_0 \Omega L p^*, \quad \alpha_m = \left(\sigma / 2 \rho \Omega \right)^{1/2} B_0, \quad E = \nu / \Omega L^2, \\ P_m = \nu / \nu_m = \sigma \mu_e \nu, \quad B_x = B'_x / \sigma \mu_e U_0 B_0 \left(\nu / \Omega \right)^{1/2}, \\ B_y = B'_y / \sigma \mu_e U_0 B_0 \left(\nu / \Omega \right)^{1/2}, \quad b_0 = b'_0 \Omega^{1/2} / \sigma \mu_e U_0 B_0 \nu^{1/2}. \end{cases}$$

Using the non-dimensional quantities defined in equation (2.8) to the equations (2.1), (2.2), (2.4) and (2.5), and combining equations (2.1) and (2.2) and equations (2.4) and (2.5), we get the following non-dimensional flow governing equations

$$(2.9) \quad \frac{\partial q}{\partial t} + 2iq = -\frac{\partial p^*}{\partial x} + E \frac{\partial^2 q}{\partial z^2} + 2\alpha_m^2 E^{1/2} \frac{\partial B}{\partial z},$$

$$(2.10) \quad P_m \frac{\partial B}{\partial t} = E^{1/2} \frac{\partial q}{\partial z} + E(1-im) \frac{\partial^2 B}{\partial z^2},$$

where $q = u + iv$ and $B = B_x + iB_y$.

The conditions to be satisfied at the boundary walls of the channel, in non-dimensional form become

$$(2.11) \quad \text{At } z = -1: q = 0, B = b_0 \left(1 + \varepsilon \left(e^{-i\omega t} + e^{i\omega t} \right) / 2 \right).$$

$$(2.12) \quad \text{At } z = 1: q = \left(1 + \varepsilon \left(e^{-i\omega t} + e^{i\omega t} \right) / 2 \right), B = b_0 \left(1 + \varepsilon \left(e^{-i\omega t} + e^{i\omega t} \right) / 2 \right).$$

Since the flow is induced due to an applied periodic pressure gradient and the oscillatory movement of the upper wall of the channel, and the walls of the channel are periodically magnetized along x' -direction. Therefore, pressure gradient, fluid velocity and the induced magnetic field may assume as

$$(2.13) \quad -\frac{\partial p^*}{\partial x} = R \left[1 + \frac{\varepsilon}{2} \left(e^{-i\omega t} + e^{i\omega t} \right) \right],$$

$$(2.14) \quad q(z, t) = q_0(z) + \frac{\varepsilon}{2} \left[q_1(z) e^{i\omega t} + q_2(z) e^{-i\omega t} \right],$$

$$(2.15) \quad B(z, t) = B_0(z) + \frac{\varepsilon}{2} \left[B_1(z) e^{i\omega t} + B_2(z) e^{-i\omega t} \right].$$

On using equations (2.13)-(2.15) to the coupled partial differential equations (2.9) and (2.10), we get the following system of ordinary differential equations

$$(2.16) \quad Eq_0'' - 2iq_0 = -R - 2\alpha_m^2 E^{1/2} B_0',$$

$$(2.17) \quad Eq_1'' - i(\omega + 2)q_1 = -2\alpha_m^2 E^{1/2} B_1' - R,$$

$$(2.18) \quad Eq_2'' + i(\omega - 2)q_2 = -2\alpha_m^2 E^{1/2} B_2' - R,$$

$$(2.19) \quad E(1 - im)B_0'' = -E^{1/2} q_0',$$

$$(2.20) \quad E(1 - im)B_1'' - iP_m \omega B_1 = -E^{1/2} q_1',$$

$$(2.21) \quad E(1 - im)B_2'' + iP_m \omega B_2 = -E^{1/2} q_2'.$$

The non-dimensional boundary conditions at the walls of the channel are

$$(2.22) \quad \text{At } z = -1: q_0 = q_1 = q_2 = 0, B_0 = B_1 = B_2 = b_0.$$

$$(2.23) \quad \text{At } z = 1: q_0 = q_1 = q_2 = 1, B_0 = B_1 = B_2 = b_0.$$

Solving equations (2.16)-(2.21) subject to the boundary conditions (2.22) and (2.23), we obtain q_0, q_1, q_2 and B_0, B_1, B_2 . Substituting q_0, q_1, q_2 and B_0, B_1, B_2 in the equations (2.14) and (2.15) respectively, we obtain the expressions for fluid velocity and induced magnetic field, which are presented in the following form

$$(2.24) \quad \left\{ \begin{aligned} q(z, t) &= \frac{1}{2} + C_1 \sinh \lambda_0 z + C_2 (\cosh \lambda_0 z - \cosh \lambda_0) \\ &+ \frac{\varepsilon}{2} \left[\left(C_3 \left(\cosh \lambda_1 z - \cosh \lambda_1 \frac{\cosh \lambda_2 z}{\cosh \lambda_2} \right) + C_4 \left(\sinh \lambda_1 z - \sinh \lambda_1 \frac{\sinh \lambda_2 z}{\sinh \lambda_2} \right) \right. \right. \\ &+ \frac{\cosh \lambda_2 z}{\cosh \lambda_2} \left(\frac{1}{2} + b_1 \right) + \frac{\sinh \lambda_2 z}{2 \sinh \lambda_2} - b_1 \Big) e^{i\omega t} + \left(C_5 \left(\cosh \lambda_3 z - \cosh \lambda_3 \frac{\cosh \lambda_4 z}{\cosh \lambda_4} \right) \right. \\ &\left. \left. + C_6 \left(\sinh \lambda_3 z - \sinh \lambda_3 \frac{\sinh \lambda_4 z}{\sinh \lambda_4} \right) + \frac{\cosh \lambda_4 z}{\cosh \lambda_4} \left(\frac{1}{2} - b_1 \right) + \frac{\sinh \lambda_4 z}{2 \sinh \lambda_4} + b_1 \right) e^{-i\omega t} \right], \end{aligned} \right.$$

$$\begin{aligned}
 (2.25) \quad & \left\{ \begin{aligned}
 & B(z,t) = \frac{1}{2\alpha_m^2 E^{1/2}} \left[\left(\frac{2i}{\lambda_0} - E\lambda_0 \right) [C_1 (\cosh \lambda_0 z - \cosh \lambda_0) + C_2 \sinh \lambda_0 z] \right. \\
 & \left. - 2C_2 iz \cosh \lambda_0 + (i - R)z + 2\alpha_m^2 E^{1/2} b_0 \right] \\
 & + \frac{\varepsilon}{2} \left[\frac{1}{iP_m \omega} \left\{ a_1 \left\{ C_3 \left(\lambda_1 \sinh \lambda_1 z - \lambda_2 \cosh \lambda_1 \frac{\sinh \lambda_2 z}{\cosh \lambda_2} \right) \right. \right. \right. \\
 & \left. \left. + C_4 \left(\lambda_1 \cosh \lambda_1 z - \lambda_2 \sinh \lambda_1 \frac{\cosh \lambda_2 z}{\sinh \lambda_2} \right) \right\} \right. \\
 & \left. - b_2 \left\{ C_3 \left(\lambda_1^3 \sinh \lambda_1 z - \lambda_2^3 \cosh \lambda_1 \frac{\sinh \lambda_2 z}{\cosh \lambda_2} \right) \right. \right. \\
 & \left. \left. + C_4 \left(\lambda_1^3 \cosh \lambda_1 z - \lambda_2^3 \sinh \lambda_1 \frac{\cosh \lambda_2 z}{\sinh \lambda_2} \right) \right. \right. \\
 & \left. \left. + \lambda_2 a_3 \left\{ \left(\frac{1}{2} + b_1 \right) \frac{\sinh \lambda_2 z}{\cosh \lambda_2} + \frac{\cosh \lambda_2 z}{2 \sinh \lambda_2} \right\} \right\} e^{i\omega t} \right. \\
 & \left. - \left(\frac{1}{iP_m \omega} \right) \left\{ a_2 \left\{ C_5 \left(\lambda_3 \sinh \lambda_3 z - \lambda_4 \cosh \lambda_3 \frac{\sinh \lambda_4 z}{\cosh \lambda_4} \right) \right. \right. \right. \\
 & \left. \left. + C_6 \left(\lambda_3 \cosh \lambda_3 z - \lambda_4 \sinh \lambda_3 \frac{\cosh \lambda_4 z}{\sinh \lambda_4} \right) \right\} \right. \\
 & \left. - b_1 \left\{ C_5 \left(\lambda_3^3 \sinh \lambda_3 z - \lambda_4^3 \cosh \lambda_3 \frac{\sinh \lambda_4 z}{\cosh \lambda_4} \right) \right. \right. \\
 & \left. \left. + C_6 \left(\lambda_3^3 \cosh \lambda_3 z - \lambda_4^3 \sinh \lambda_3 \frac{\cosh \lambda_4 z}{\sinh \lambda_4} \right) \right. \right. \\
 & \left. \left. + \lambda_4 a_4 \left\{ \left(\frac{1}{2} - b_1 \right) \frac{\sinh \lambda_4 z}{\cosh \lambda_4} + \frac{\cosh \lambda_4 z}{2 \sinh \lambda_4} \right\} \right\} e^{-i\omega t} \right].
 \end{aligned}
 \right.
 \end{aligned}$$

3. Skin Friction at the Walls

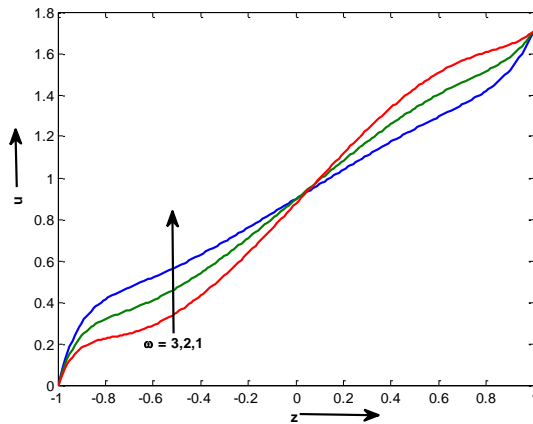
The skin friction at the walls of the channel are given by

$$(3.1) \quad \left\{ \begin{aligned} & (\tau_x + i\tau_y)_{z=\pm 1} \\ & = C'_1 \lambda_0 \cosh \lambda_0 \pm C'_2 \lambda_0 \sinh \lambda_0 + \frac{\varepsilon}{2} \left[(\pm C'_3 (\lambda_1 \sinh \lambda_1 - \lambda_2 \cosh \lambda_1 \tanh \lambda_2) \right. \\ & \left. + C'_4 (\lambda_1 \cosh \lambda_1 - \lambda_2 \sinh \lambda_1 \coth \lambda_2) \pm \lambda_2 \tanh \lambda_2 \left(\frac{1}{2} + b_2 \right) + \frac{\lambda_2 \coth \lambda_2}{2} \right) e^{i\omega t} \\ & \pm (C'_5 (\lambda_3 \sinh \lambda_3 - \lambda_4 \cosh \lambda_3 \tanh \lambda_4) + C'_6 (\lambda_3 \cosh \lambda_3 - \lambda_4 \sinh \lambda_3 \coth \lambda_4) \\ & \left. \pm \lambda_4 \tanh \lambda_4 \left(\frac{1}{2} - b_2 \right) + \frac{\lambda_4 \coth \lambda_4}{2} \right) e^{-i\omega t} \right]. \end{aligned} \right.$$

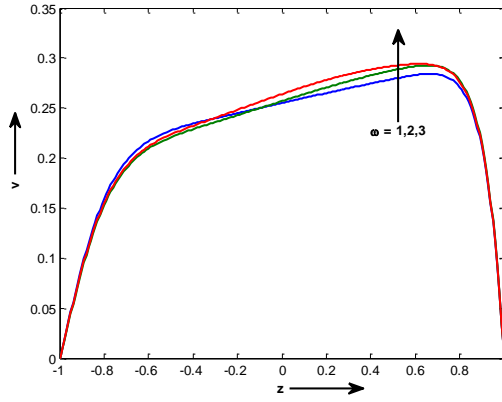
4. Numerical Results and Discussion

To analyze the flow behavior, the analytical solutions for fluid velocity (2.24) and induced magnetic field (2.25) are numerically computed and presented in graphical form whereas the skin friction at the moving upper wall of the channel is numerically computed and presented in tabular form. In numerical computation we have taken $R = 1$, $\varepsilon = 1$ and $b_0 = 1$. Figures 1-5 depict the velocity profiles whereas figures 6 to 10 display the induced magnetic field profiles for various values of flow governing parameters.

Figures 1 demonstrate the influence of oscillations ω on velocity profiles. It is noticed that, on raising frequency of oscillations, the fluid velocity in both the primary and secondary directions rising in the upper half of the channel while this effect is upturned in the lower half of the channel. This is due to the oscillation of the upper wall of the channel.

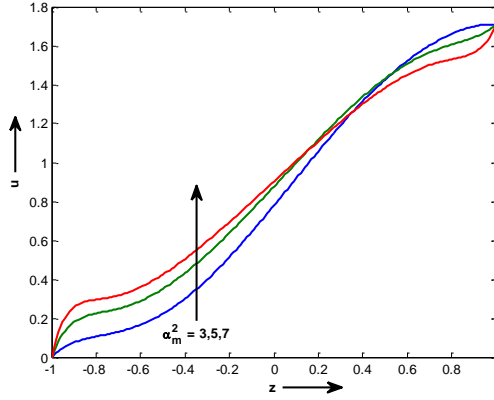


(a)

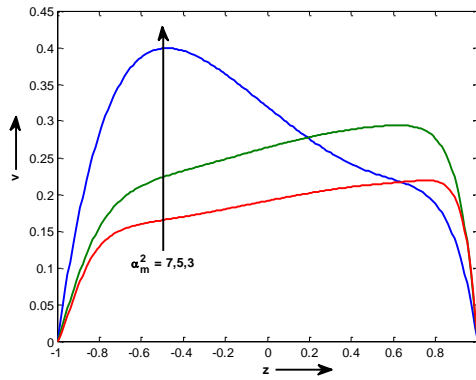


(b)

Fig. 1 Velocity profiles in the (a) primary and (b) secondary flow directions when $\alpha_m^2 = 5$, $m = 0.5$, $E = 0.5$, $P_m = 0.7$, $R = 1$ and $\omega t = \pi / 4$.



(a)



(b)

Fig. 2 Velocity profiles in the (a) primary and (b) secondary flow directions when $\omega = 3$, $m = 0.5$, $E = 0.5$, $P_m = 0.7$, $R = 1$ and $\omega t = \pi / 4$.

Figures 2 display applied magnetic field effects on the velocity profiles. It can be easily seen from figures 2 that, the fluid velocity in the primary flow direction rises on raising magnetic interaction parameter α_m^2 in most of the lower half of the channel while this effect is upturned in the vicinity of the upper wall of the channel. Magnetic field shows the reverse behavior on the fluid velocity in the secondary flow direction as that of the fluid velocity in the primary flow direction.

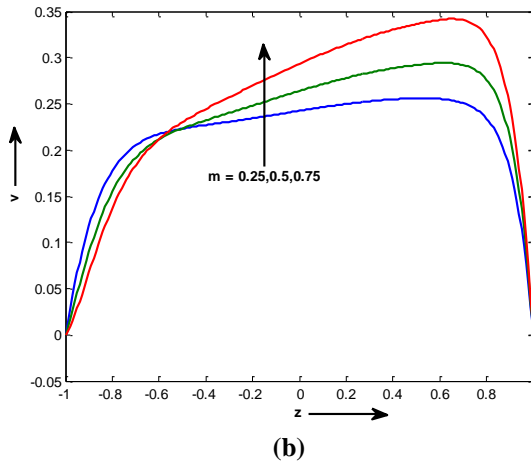
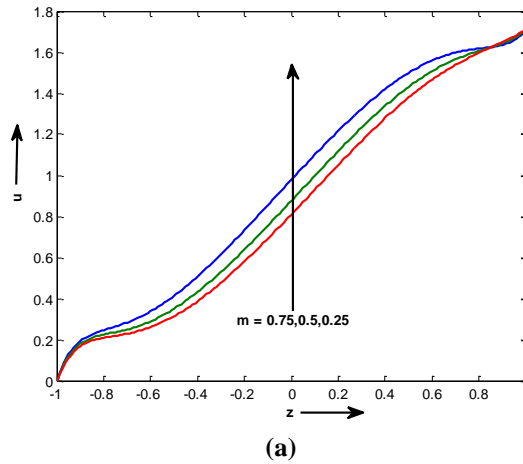
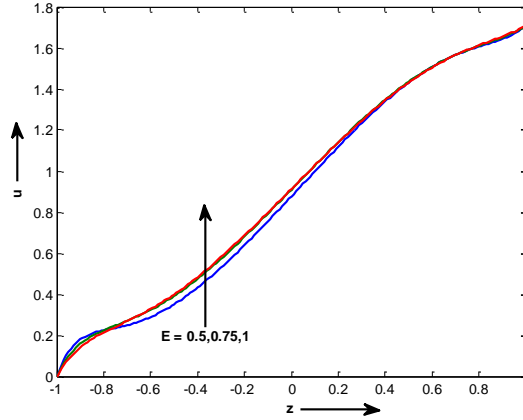


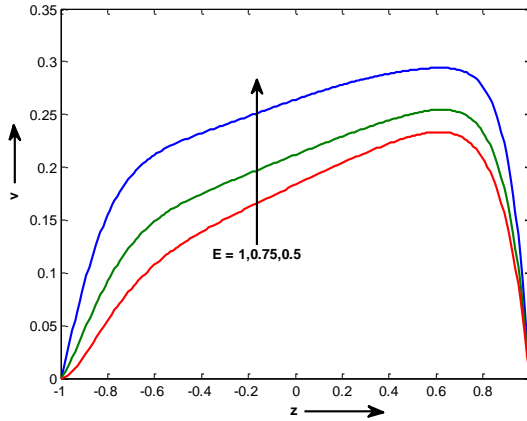
Fig. 3 Velocity profiles in the (a) primary and (b) secondary flow directions when $\omega = 3$, $\alpha_m^2 = 5$, $E = 0.5$, $P_m = 0.7$, $R = 1$ and $\omega t = \pi / 4$.

Hall current effects on the velocity distributions are depicted in

figures 3. Figures 3 show that Hall current decelerates the fluid velocity in the primary flow direction throughout the channel except a thin region in the vicinity of the upper wall. On raising Hall current, the fluid velocity in the secondary flow direction rise in most of the upper half of the channel while this effect is upturned in the vicinity of the lower half of the channel.



(a)



(b)

Fig. 4 Velocity profiles in the (a) primary and (b) secondary flow directions when $\omega = 3, \alpha_m^2 = 5, m = 0.5, P_m = 0.7, R = 1$ and $\omega t = \pi / 4$.

Figures 4 demonstrate the effect of Ekman number E (rotation) on the velocity profiles. The velocity profiles in the primary flow direction are of oscillatory nature on increasing Ekman number. The velocity profiles in the secondary flow direction falls on raising Ekman number i.e. fluid velocity in the secondary flow direction rise on raising angular

velocity of rotation Ω because angular velocity of rotation has an inverse relation with Ekman number. Our result is in agreement with the well accepted result that rotation induces motion in the secondary flow direction.

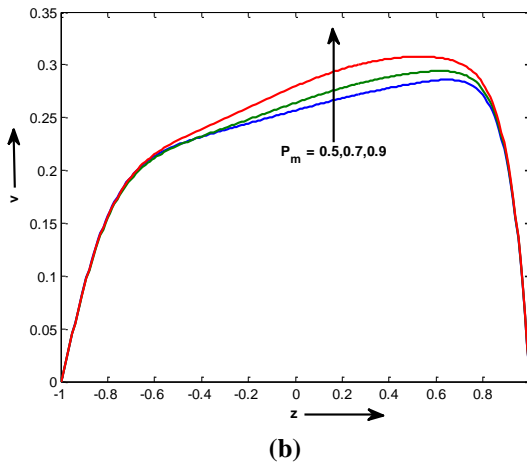
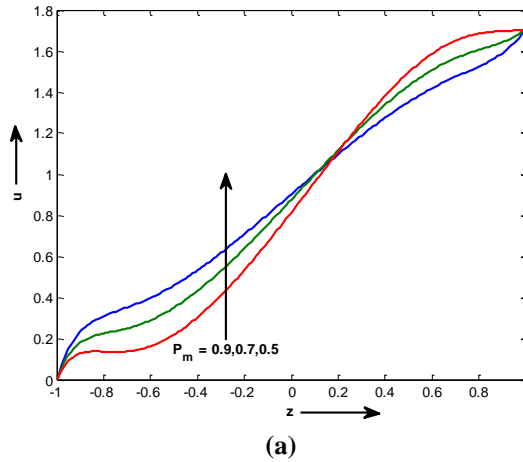


Fig. 5 Velocity profiles in the (a) primary and (b) secondary flow directions when $\omega = 3, \alpha_m^2 = 5, m = 0.5, E = 0.5, R = 1$ and $\omega t = \pi / 4$.

The variations of the velocity profiles for various values of magnetic Prandtl number P_m are displayed in figures 5. It is observed that the fluid velocity in the secondary flow direction and fluid velocity in the primary flow direction in the upper half of the channel rise on raising magnetic Prandtl number while this effect on the fluid velocity in the primary flow direction is upturned in the lower half of the channel. Since the magnetic

diffusivity has an inverse relation with magnetic Prandtl number, thus magnetic diffusivity has tendency to reduce fluid velocity in the secondary flow direction and fluid velocity in the primary flow direction in the upper half of the channel.

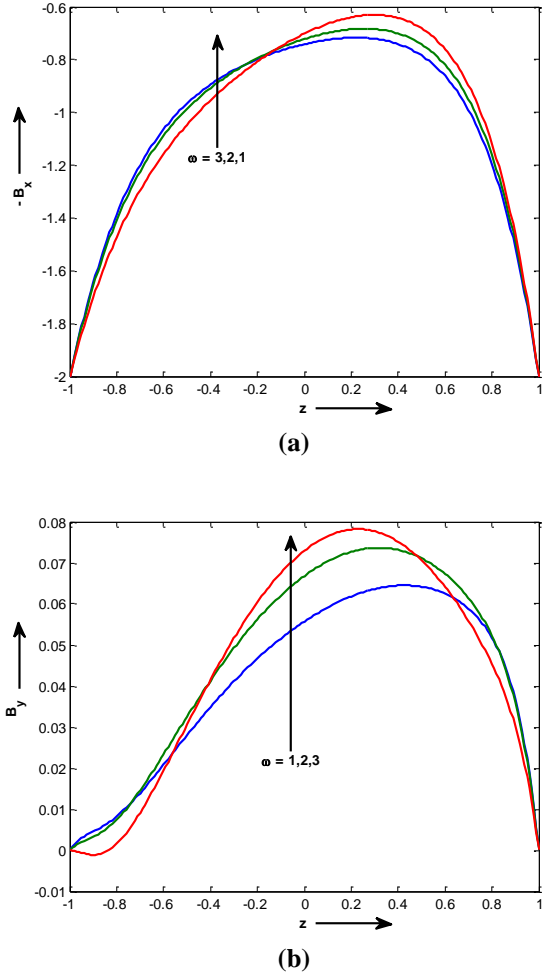
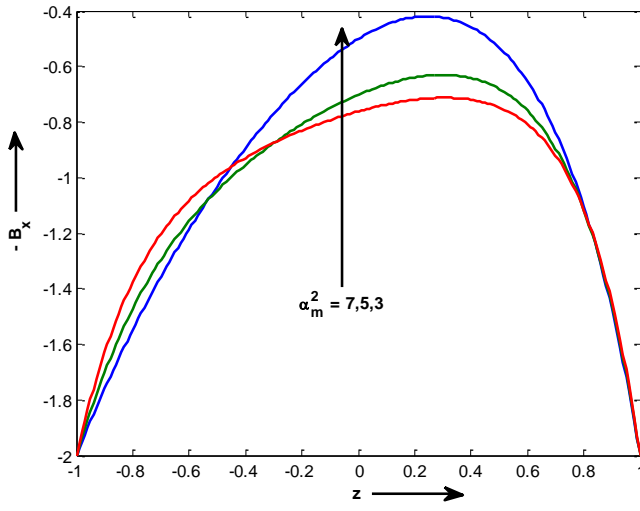
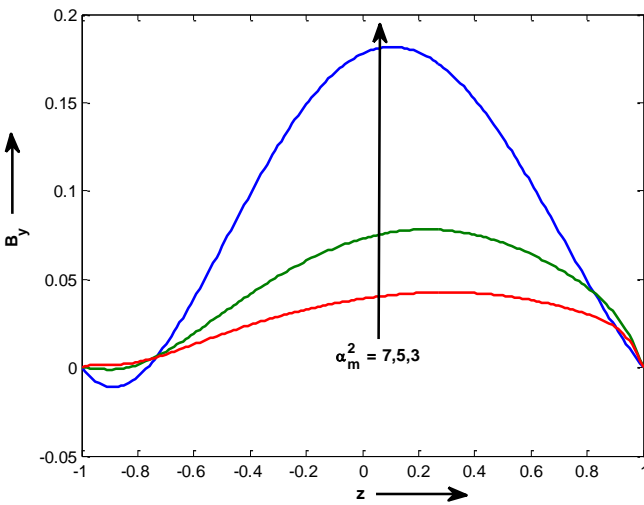


Fig. 6 Induced magnetic field profiles in the (a) primary and (b) secondary flow directions when $\alpha_m^2 = 5$, $m = 0.5$, $E = 0.5$, $P_m = 0.7$, $R = 1$ and $\omega t = \pi / 4$.

Figures 6 show the influence of oscillations on the induced magnetic field. The induced magnetic field in the primary flow direction rises on raising frequency of oscillations in the upper half of the channel while this effect is upturned in the lower half of the channel. Oscillations show the oscillatory nature on induced magnetic field in the secondary flow direction.



(a)



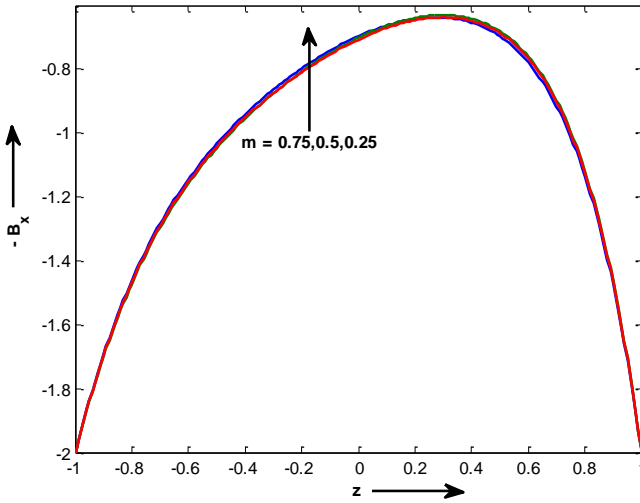
(b)

Fig. 7 Induced magnetic field profiles in the (a) primary and (b) secondary flow directions when $\omega = 3$, $m = 0.5$, $E = 0.5$, $P_m = 0.7$, $R = 1$ and $\omega t = \pi / 4$.

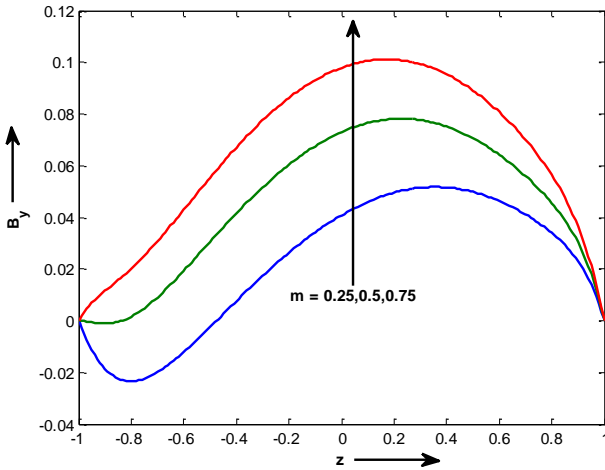
Deviation in the induced magnetic field profiles for various values of magnetic interaction parameter are presented in figures 7. It can be noticed that magnetic field tends to raise induced magnetic field in the primary flow direction in the neighborhood of the lower wall of the channel while this effect is upturned in most of the upper half region of the channel. Induced magnetic field in the secondary flow direction reduces throughout

the channel except in the vicinity of the upper wall.

Figures 8 display the variation of induced magnetic field profiles for various values of Hall current. Hall current has tendency to reduce induced magnetic field in the lower half of the channel while this effect is upturned in the upper half of the channel.

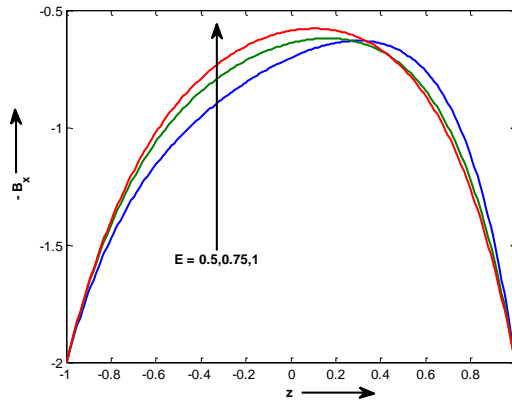


(a)

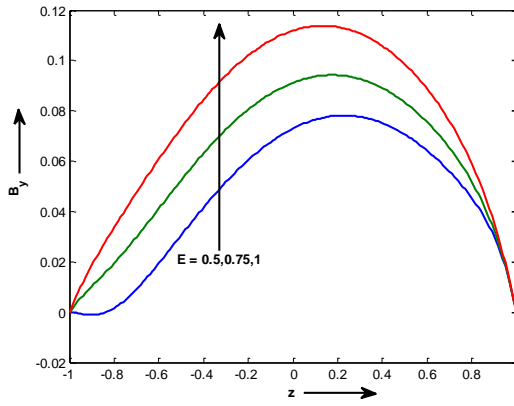


(b)

Fig. 8 Induced magnetic field profiles in the (a) primary and (b) secondary flow directions when $\omega = 3$, $\alpha_m^2 = 5$, $E = 0.5$, $P_m = 0.7$, $R = 1$ and $\omega t = \pi / 4$.

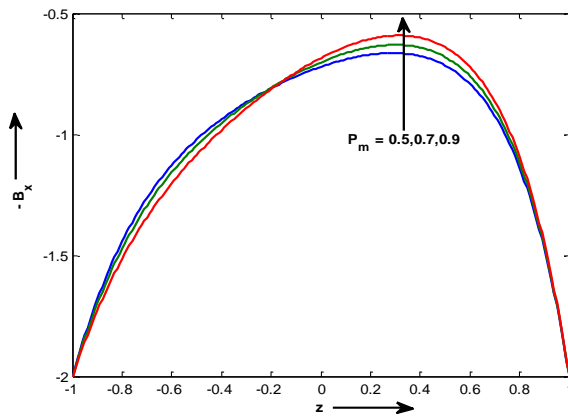


(a)



(b)

Fig. 9 Induced magnetic field profiles in the (a) primary and (b) secondary flow directions when $\omega = 3$, $\alpha_m^2 = 5$, $m = 0.5$, $P_m = 0.7$, $R = 1$ and $\omega t = \pi / 4$.



(a)

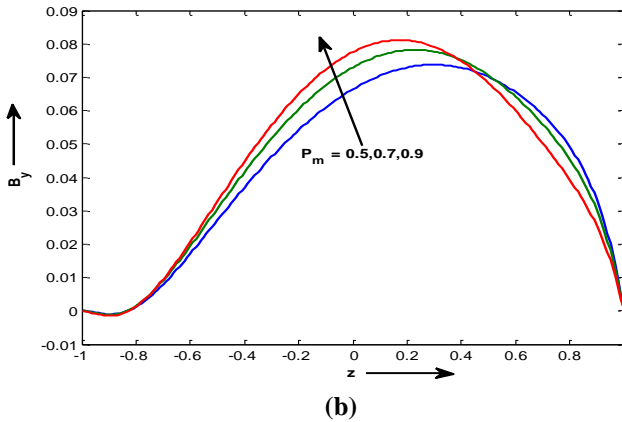


Fig. 10 Induced magnetic field profiles in the (a) primary and (b) secondary flow directions when $\omega = 3, \alpha_m^2 = 5, m = 0.5, E = 0.5, R = 1$ and $\omega t = \pi / 4$.

Effect of rotation on induced magnetic field is demonstrated in figures 9. Rotation tends to raise the induced magnetic field in the primary flow direction in the upper half region of the channel while this effect is reversed on the induced magnetic field in the secondary flow direction and induced magnetic field in the primary flow direction in the upper half of the channel.

Influences of magnetic diffusivity on induced magnetic field are shown in figures 10. It is seen that magnetic diffusivity tends to rise induced magnetic field in the primary flow direction in the lower half of the channel while this effect is upturned in the upper half of the channel. Magnetic diffusivity shows the reverse behavior on the induced magnetic field in the secondary flow direction as that of on the primary flow direction.

The variations of the skin friction at the moving wall for various values of flow governing parameters are presented in table 1. It can be noted that oscillations and rotation tend to reduce skin friction in the primary flow direction while magnetic field, rotation, Hall current and magnetic diffusivity tend to rise the skin friction in the secondary flow direction.

Table 1 Skin friction at the moving wall of the channel.

ω	α_m^2	E	m	P_m	Skin friction at the moving wall	
					τ_x	τ_y
1	5	0.5	0.5	0.7	2.4162	3.5150
2	5	0.5	0.5	0.7	1.3475	3.5051
3	5	0.5	0.5	0.7	0.0456	3.6946
3	3	0.5	0.5	0.7	-0.5898	2.9152
3	7	0.5	0.5	0.7	2.1782	3.8896

3	5	0.75	0.5	0.7	0.3483	2.5677
3	5	1	0.5	0.7	0.3797	2.1018
3	5	0.5	0.25	0.7	0.1980	2.8855
3	5	0.5	0.75	0.7	-0.1452	4.2162
3	5	0.5	0.5	0.5	1.1739	3.4717
3	5	0.5	0.5	0.9	-0.8363	4.4226

5. Conclusions

A mathematical analysis has been presented for unsteady MHD generalized Couette flow of an incompressible and electrically conducting fluid in a rotating channel with induced magnetic field and Hall current. The influence of some significant flow governing parameters on the flow variables have been thoroughly discussed in the previous section. Some significant findings are summarized below:

- (i) On rising Hall current, the fluid velocity in the secondary flow direction raise in most of the upper half region of the channel while this effect is upturned in the vicinity of the lower half of the channel. Hall current has tendency to reduce induced magnetic field in the lower half of the channel while this effect is upturned in the upper half of the channel.
- (ii) The magnetic diffusivity has tendency to reduce fluid velocity in the secondary flow direction and fluid velocity in the primary flow direction in the upper half of the channel. Magnetic diffusivity tends to rise induced magnetic field in the primary flow direction in the lower half of the channel while this effect is upturned in the upper half of the channel. Magnetic diffusivity shows the reverse behavior on the induced magnetic field in the secondary flow direction as that of on the primary flow direction.

Appendix

$$a_1 = \left(E^{1/2} + \frac{E(1-im)}{2\alpha_m^2 E^{1/2}} i(\omega + 2) \right), a_2 = \left(E^{1/2} - \frac{E(1-im)}{2\alpha_m^2 E^{1/2}} i(\omega + 2) \right),$$

$$a_3 = \left(E^{1/2} - \frac{E(1-im)}{2\alpha_m^2 E^{1/2}} (E\lambda_2^2 - i(\omega + 2)) \right), a_4 = \left(E^{1/2} - \frac{E(1-im)}{2\alpha_m^2 E^{1/2}} (E\lambda_4^2 + i(\omega + 2)) \right),$$

$$b_1 = \frac{iR}{(\omega + 2)}, b_2 = \frac{E^2(1-im)}{2\alpha_m^2 E^{1/2}}, p_1 = i \left(\frac{\omega P_m (1+im)(\omega + 2)}{(1+m^2)} \right)^{1/2},$$

$$n_1 = \frac{1}{2} \left\{ \left(\frac{2\alpha_m^2}{(1+m^2)} - \frac{\omega m P_m}{(1+m^2)} \right) + i \left(2 + \omega \left(1 + \frac{P_m}{(1+m^2)} \right) + \frac{2m\alpha_m^2}{(1+m^2)} \right) \right\},$$

$$n_2 = \frac{1}{2} \left\{ \left(\frac{2\alpha_m^2}{(1+m^2)} + \frac{\omega m P_m}{(1+m^2)} \right) - i \left(-2 + \omega \left(1 + \frac{P_m}{(1+m^2)} \right) - \frac{2m\alpha_m^2}{(1+m^2)} \right) \right\},$$

$$\lambda_0 = E^{-1/2} \left\{ \frac{2\alpha_m^2}{(1+m^2)} + i \left(2 + \frac{2m\alpha_m^2}{(1+m^2)} \right) \right\}^{1/2}, \quad \lambda_1, \lambda_2 = E^{-1/2} \left\{ n_1 \pm (n_1^2 - p_1^2)^{1/2} \right\}^{1/2},$$

$$p_2 = i \left(\frac{\omega P_m (1+im)(\omega-2)}{(1+m^2)} \right)^{1/2}, \quad \lambda_3, \lambda_4 = E^{-1/2} \left[n_2 \pm (n_2^2 - p_2^2)^{1/2} \right]^{1/2}, \quad C_1 = \frac{1}{2 \sinh \lambda_0},$$

$$C_2 = \left(\frac{(R-i)\lambda_0}{(2i - E\lambda_0^2) \sinh \lambda_0 - 2i\lambda_0 \cosh \lambda_0} \right),$$

$$C_3 = - \frac{(1+2b_2)\lambda_2 \tanh \lambda_2 a_3}{2 \left[(\lambda_1 \sinh \lambda_1 - \lambda_2 \cosh \lambda_1 \tanh \lambda_2) a_1 - b_1 (\lambda_1^3 \sinh \lambda_1 - \lambda_2^3 \cosh \lambda_1 \tanh \lambda_2) \right]},$$

$$C_4 = \frac{2iP_m \omega b_0 - \lambda_2 \cosh \lambda_2 a_3}{2 \left[(\lambda_1 \cosh \lambda_1 - \lambda_2 \sinh \lambda_1 \coth \lambda_2) a_1 - b_1 (\lambda_1^3 \cosh \lambda_1 - \lambda_2^3 \sinh \lambda_1 \coth \lambda_2) \right]},$$

$$C_5 = - \frac{(1+2b_2)\lambda_4 \tanh \lambda_4 a_4}{2 \left[(\lambda_3 \sinh \lambda_3 - \lambda_4 \cosh \lambda_3 \tanh \lambda_4) a_2 - b_1 (\lambda_3^3 \sinh \lambda_3 - \lambda_4^3 \cosh \lambda_3 \tanh \lambda_4) \right]},$$

$$C_6 = \frac{-2iP_m \omega b_0 - \lambda_4 \cosh \lambda_4 a_4}{2 \left[(\lambda_3 \cosh \lambda_3 - \lambda_4 \sinh \lambda_3 \coth \lambda_4) a_2 - b_1 (\lambda_3^3 \cosh \lambda_3 - \lambda_4^3 \sinh \lambda_3 \coth \lambda_4) \right]}$$

References

1. Y. S. Muzychka and M. M. Yovanovich, Unsteady viscous flows and Stokes first problem, *Proc. IMECE*, **14301** (2006) 1-11.
2. J. P. Agarwal, On generalized incompressible Couette flow in hydromagnetics, *Appl. Sci. Res.*, **9(4)** (1961) 255-266.
3. V. M. Soundalgekar, On generalised MHD Couette flow with heat transfer, *Proc. Indian Acad. Sci.*, **64(5)** (1966) 304-314.

4. O. A. Beg, J. Zuco and H. S. Takhar, Unsteady magnetohydrodynamic Hartmann–Couette flow and heat transfer in a Darcian channel with Hall current, ion-slip, viscous and Joule heating effects: Network numerical solutions, *Comm. Nonlin. Sci. Num. Sim.*, **14(4)** (2009) 1082-1097.
5. J. K. Singh, N. Joshi and S. G. Begum, Unsteady magnetohydrodynamic Couette-Poiseuille flow within porous plates filled with porous medium in the presence of a moving magnetic field with Hall and ion-slip effects, *Int. J. Heat and Tech.*, **34(1)** (2016) 89-97.
6. J. K. Singh, S. G. Begum and N. Joshi, Unsteady MHD Couette-Hartmann flow through a porous medium bounded by porous plates with Hall current, ion-slip and Coriolis effects, *Int. J. Industrial Mathematics*, **8(4): IJIM-00727** (2016) 14 pages.
7. G. S. Seth, S. Sarkar and O. D. Makinde, Combined free and forced convection Couette-Hartmann flow in a rotating channel with arbitrary conducting walls and Hall effects, *J. Mech.*, **32(5)** (2016) 613-629.
8. T. Nagy and Z. Demendy, Effects of Hall currents and Coriolis force on Hartmann flow under general wall conditions, *Acta Mechanica*, **113(1)** (1995) 77-91.
9. B. K. Jha and C. A. Apere, Time dependent MHD Couette flow rotating fluid with Hall and ion-slip currents, *Appl. Math. Mech.*, **33(4)** (2012) 399-410.
10. K. D. Singh and R. Pathak, Effect of rotation and Hall current on mixed convection MHD flow through a porous medium filled in a vertical channel in presence of thermal radiation, *Indian J. Pure Appl. Phys.*, **50** (2012) 77-85.
11. D. Srinivasacharya and K. Kaladhar, Mixed convection flow of couple stress fluid between parallel vertical plates with Hall and ion-slip effects, *Comm. Nonlin. Sci. Num. Sim.*, **17(6)** (2012) 2447-2462.
12. S. Das, R. N. Jana and O. D. Makinde, An oscillatory MHD convective flow in a vertical channel filled with porous medium with Hall and thermal radiation effects, *Special Topics & Reviews in Porous Media: An International Journal*, **5(1)** (2014) 63-82.
13. G. S. Seth and J. K. Singh, Mixed convection hydromagnetic flow in a rotating channel with Hall and wall conductance effects, *Appl. Math. Mod.*, **40(4)** (2016) 2783-2803.
14. S. K. Ghosh and P. K. Bhattacharjee, Magnetohydrodynamic convective flow in a rotating channel, *Arch. Mech.*, **52(2)** (2000) 303-318.
15. Md. S. Ansari, G. S. Seth and R. Nandkeolyar, Unsteady Hartmann flow in a rotating channel with arbitrary conducting walls, *Math. Compt. Mod.*, **54** (2011) 765-779.
16. G. S. Seth, J. K. Singh, N. Mahto and N. Joshi, Oscillatory Hartmann flow in rotating channel with magnetized walls, *Mathematical Sciences Letters*, **5(3)** (2016) 259-269.